Journal of Theoretical Biology 370 (2015) 1–10

Contents lists available at ScienceDirect

Journal of Theoretical Biology

journal homepage: www.elsevier.com/locate/yjtbi

Motor function in interpolar microtubules during metaphase

J.M. Deutsch*, Ian P. Lewis

Department of Physics, University of California, Santa Cruz, CA 95064, United States

HIGHLIGHTS

- We examine the mechanism that results in constant spindle spacing during prometaphase.
- We analyze *in vitro* gliding assays of two antagonistic motors related to this process.
- Microtubule motion ceases with the right balance of these motor species.
- We show that these results can be explained by considering concentration fluctuations.
- These fluctuations pin the microtubule to points where it can only jitter randomly.

ARTICLE INFO

Article history:
Received 17 July 2014
Received in revised form
4 December 2014
Accepted 12 January 2015
Available online 19 January 2015

Keywords:
Random walks
Stochastic modeling
Fluctuations
Motility assays
Mitotic spindle

ABSTRACT

We analyze experimental motility assays of microtubules undergoing small fluctuations about a "balance point" when mixed in solution of two different kinesin motor proteins, KLP61F and Ncd. It has been proposed that the microtubule movement is due to stochastic variations in the densities of the two species of motor proteins. We test this hypothesis here by showing how it maps onto a one-dimensional random walk in a random environment. Our estimate of the amplitude of the fluctuations agrees with experimental observations. We point out that there is an initial transient in the position of the microtubule where it will typically move of order its own length. We compare the physics of this gliding assay to a recent theory of the role of antagonistic motors on restricting interpolar microtubule sliding of a cell's mitotic spindle during prometaphase. It is concluded that randomly positioned antagonistic motors can restrict relative movement of microtubules, however they do so imperfectly. A variation in motor concentrations is also analyzed and shown to lead to greater control of spindle length.

1. Introduction

During mitosis, pole spacing is regulated by a system of interpolar microtubules. It has been proposed that the interpolar microtubules can be moved in two directions by opposing motors (Heck et al., 1993; Cole et al., 1994; Cottingham et al., 1999; Enos and Morris, 1990; Saunders and Hoyt, 1992; Sawin et al., 1992; Straight et al., 1998), but the details of such a proposed system are not yet well understood (Sharp et al., 1999; Brust-Mascher and Scholey, 2002). The interpolar microtubules are likely bundled and moved by two families of kinesin motor proteins; kinesin-5 and kinesin-14. Experiments with *Drosophila melanogaster* suggest that a kinesin-5 motor protein, KLP61F, plays a large role in creating the spindle during prometaphase (Heck et al., 1993). It has also been shown that kinesin-5 forms cross-bridges between interpolar microtubules in the centralspindlin (Sharp et al., 1999). Further experiments suggest that the same motor drives the separation of the poles during metaphase and anaphase (Brust-Mascher and Scholey, 2002; Tao et al., 2006a). In vitro experiments show that KLP61F slides antiparallel microtubules apart on motility assays, where motor proteins are bound to glass slides and move microtubules that are added to the solution (Tao et al., 2006a).

All of the above results show that kinesin-5 plays an important role in controlling the spindle spacing. Being a tetramer with both dimers at the N-terminus, the motor can walk toward the plus ends of two antiparallel microtubules, thus forcing the poles apart.

The kinesin-5 are antagonized by the kinesin-14, which walk toward the minus end of the microtubules. In vitro experiments show that a kinesin-14, Ncd, is capable of bundling microtubules and driving an inward sliding of the interpolar microtubules (Sharp et al., 1999). With one motor able to separate the poles, and one able to bring them closer, it seems possible that the two motors are responsible for maintaining spindle spacing and moving the poles apart. The net force exerted by the two motor species could govern the direction and rate of pole movement.

Recently, seminal work has been done in trying to understand how outward microtubule sliding generated by the kinesin-5 and inward

* Corresponding author.
E-mail addresses: josh@ucsc.edu (J.M. Deutsch), ianpeterlewis@gmail.com (I.P. Lewis).

http://dx.doi.org/10.1016/j.jtbi.2015.01.011
0022-5193/

sliding generated by the kinesin-14 could result in the stable, steady-state spindle spacing during prometaphase. A balance of forces could result in a stationary spindle, but it is unclear how the "collective antagonism" could occur (Tao et al., 2006a). In the following section, we will discuss one group's proposed solution to the problem.

1.1. Experimental work

Experiments with in vitro motility assays were performed to see if KLP61F and Ncd could interact to control the speed and polarity of microtubules' motility and whether the antagonism between the motors could stall microtubule sliding enough to produce the stable steady-state spindle spacing observed during prometaphase (Tao et al., 2006a). Before combining both motors in an assay, each motor was observed moving microtubules in motility assays as expected. KLP61F moved microtubules at 0.04 μm/s with the minus ends leading and Ncd moved microtubules at 0.1 μm/s with the plus ends leading (Tao et al., 2006a). Further experiments also showed that KLP61F alone, Ncd alone, and mixtures of the two motors bundled microtubules under conditions with physiological ATP concentrations (Tao et al., 2006a).

To see how the two species of motors would interact, different molar ratios of KLP61F and Ncd were mixed and microtubule motility was measured. A balance point at a mole fraction of 0.7 Ncd was found where microtubules displayed a mean velocity of approximately zero (Tao et al., 2006a). For greater mole fractions of Ncd, the mean velocity was plus end directed. Conversely, for smaller mole fractions of Ncd, the mean velocity was minus end directed, as shown in Fig. 5(a) of Tao et al. (2006a). The slope of the lines fit to the two sides of the balance point in this figure suggests that KLP61F is a strong, slow motor that is not slowed down easily by the weak, fast Ncd motor, which in turn is slowed down easily by KLP61F (Tao et al., 2006a). At the balance point, the microtubules were observed to display oscillatory motion between KLP61F and Ncd directed movement with intermediate rates of roughly 0.02 μm/s, as shown in Fig. 5(b) of Tao et al. (2006a). This is reproduced in Fig. 1(a), and the initial transient behavior is shown in Fig. 1(b).

Tao et al. (2006a) suggest that KLP61F and Ncd motors could act synchronously to antagonize one another. However, being an inherently stochastic process, it is hard to see how motor power stroking could become synchronized. In later work (Civelekoglu-Scholey et al., 2010), a fully stochastic force dependent detachment rate (FDDR) model was devised and tested numerically, and the synchronization was made more physically viable by a detailed model of the two motors' response to force and displacement. The model incorporates stochastic binding of a number of antagonistic motors to microtubules. One motor will "win" over the other kind, leading to motion in that direction. The losing motor will continue to try to bind to the microtubule, however the model posits a detachment rate that depends strongly on the force applied. Above some threshold force, these motors only bind for short times before detaching. This implies that once a direction has been chosen, it is hard for the losing motor to oppose this motion. Simulations show that only occasional changes in the sign of velocity can occur, on the scale of hundreds of seconds, happening only when an unlikely circumstance allows the losing motors to gain control. This kind of bistability in directionality has been considered before in the case of a single motor (Jülicher and Prost, 1995, 1997; Duke, 2002; Guérin et al., 2010), and also with antagonistic interactions (Gilboa et al., 2009). Therefore there are systems where this kind of behavior is well established. In order for this to be a viable explanation, first, the size of stochastic fluctuations has to be large enough to allow switching between the two opposing states (Badoual et al., 2002). Second, because the position of the microtubule remains constant during prometaphase, while additional forces act on it, the position of the microtubule should remain almost constant under the application of a small but finite force. We will discuss to what extent this bistability can explain this requirement in the following section.

In addition to bistability, Tao et al. (2006a) made the important observation that microtubules could be gliding on a spatially varying landscape, with varying densities of KLP61F and Ncd motors (Tao et al., 2006a). Periods of directional movement would be due to the patches in the environment where one motor is dominant. It is possible that the microtubule finds a "valley" in the landscape where it oscillates between patches of motors that move it back towards the balance point. It is this idea that we will attempt to model in the following section.

We show that the phenomenon is quite general and independent of the details in the parameters. If the system is rescaled to be dimensionless in length and time, we find that the behavior is only controlled by one parameter; the effective "temperature" of the system. A detailed understanding of the motors will only change this effective temperature and nothing else, since scaling laws for spatio-temporal fluctuations are universal. A study from this perspective also elucidates other aspects of this system, such as the nature of initial transients in motion of the microtubules in these assays before they reach a quasi-steady state. These transients have interesting implications, as we show that they also should occur for interpolar microtubules during metaphase.

2. Physical analysis of antagonistic motor assay

2.1. Average force-velocity dependence of antagonistic motors

We first consider the problem of a single molecular motor, such as kinesin, with the tail tethered to a substrate such as a glass plate

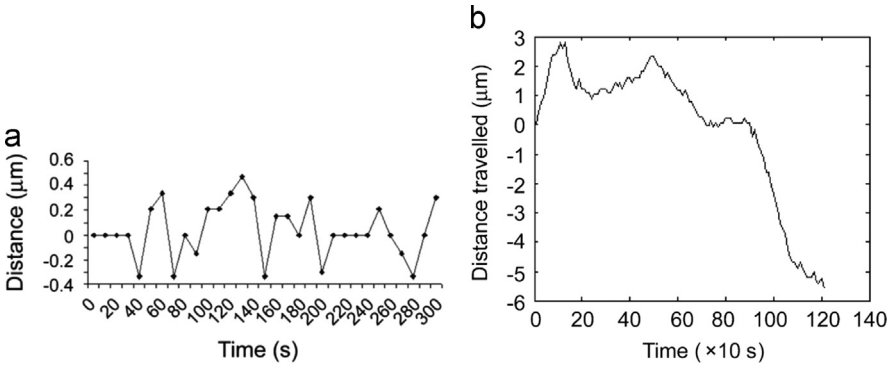

Fig. 1. (a) Plot of displacements versus time for a typical microtubule at the balance point. Reproduction of Fig. 5B from Tao et al. (2006a). (b) Initial transient behavior of this system. Reproduction of Fig. S3A from Tao et al. (2006a).

while the heads can freely interact with a long microtubule, as shown in Fig. 2. The microtubule is being moved along a single dimension at uniform velocity v that is parallel to the glass. The heads bind and unbind with the microtubule, applying an average net force f, that will depend on v. The averaging is being done over time, and we are considering the limit where the time interval goes to infinity.

Now consider a collection of N identical motors that all interact with the same microtubule but are sufficiently distant from each other that they can be considered independent. Then the average force acting on the microtubule due to these motors is $N f$.

The above analysis is easily extended to the case of two separate species of antagonistic motors, labeled 1 and 2, with average force versus velocity curves $f_1(v)$ and $f_2(v)$ respectively, as shown in Fig. 3(a). If the number of motors of each kind is N_1 and N_2, then the time averaged force is $N_1 f_1 - N_2 f_2$, where we have adopted a sign convention so that the net force is a difference, rather than a sum. If we choose the ratio $N_1/N_2 = f_2(0)/f_1(0)$, then this net average force vanishes at $v=0$. This is the "balance point" where there is no net average force acting on the microtubule. The difference between f_1 and f_2, $\Delta f(v)$, weighted in this way is shown in Fig. 3(a).

Note that for small velocities at the balance point, Fig. 3(a), the net effect of these motors is to give linear drag, because both species of motor have a linear relationship between force and velocity in this regime. This linearity breaks down at high velocities, however, as we will see below, we are interested in the low velocity regime. In this case, the net force f_{net} is proportional to Δf so that

$$f_{net} = -\gamma v, \tag{1}$$

where γ is the drag coefficient.

We note that the assumption of a monotonic force versus velocity curve, even for a single motor species, can sometimes fail (Jülicher and Prost, 1995, 1997; Duke, 2002; Guérin et al., 2010). The force–velocity curve can have the property that the slope around the origin is *positive* and there are two stable points where the force is zero, one for positive and one for negative velocities as shown in Fig. 3(b). This can occur with systems with a mixture of different polarities (Gilboa et al., 2009). In fact, the force dependent detachment rate model (Civelekoglu-Scholey et al., 2010) is also bistable.

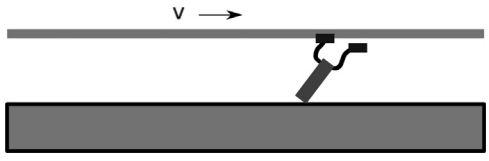

Fig. 2. A single motor with the lower end anchored against a glass plate, with its heads binding and unbinding with a microtubule that is being moved at a constant velocity v relative to the plate.

The two bistable states move in opposite directions with the same applied force. The relative prevalence of the two states, and their velocities, depend on this force. If many such motors are simultaneously attached to a microtubule, and are allowed to pull it freely, this can lead to the microtubule moving in one direction for a long time and then occasionally, due to the collective fluctuation of all the motors, reversing its direction of motion. In Fig. 3(b), these two states are shown by the black circles.

In the case of the FDDR model (Civelekoglu-Scholey et al., 2010), or any model showing bistability, if we apply an external force, the switching between states must occur on a small enough timescale so as to be compatible with experimental observation. If we average for times much longer than this switching time, the bistable curve will average to a monotonic force–velocity curve (Fig. 3(b) blurred gray line). At the balance point, the curve will intersect the origin, and look similar to Δf in Fig. 3(a). For small velocities, this gives the viscous drag behavior of Eq. (1). This will only lead to a cessation in movement under the application of additional forces if the drag coefficient γ is sufficiently large. On the other hand, as we shall show, random variations in motor density lead instead to minima in the potential energy landscape, which more easily prevent motion of microtubules acted on by forces. Thus the breaking of translational symmetry can pin a microtubule to specific locations. Without such symmetry breaking, no pinning can occur and the only effect of antagonistic motor dynamics is to modify the drag coefficient.

Formulating this problem in terms of force–velocity curves, as we have just done, is important for two reasons. First, it relates precisely the force versus velocity curve for assays containing a motor mixture at arbitrary concentration to the behavior of single motor assays. Empirical data on single motor assays can be obtained and then used to understand average properties of these mixed systems. Second, it shows that at the balance point there is only one parameter that needs to be characterized in order to understand observations; the drag coefficient γ.

Now that we have understood the behavior of the average force, we shall turn our attention to the effects of spatio-temporal fluctuations on the motion of microtubules. As we shall see, these fluctuations are crucial to understanding the system's behavior.

2.2. The effect of spatiotemporal fluctuations

We will consider a system at the balance point, where the concentrations of the two antagonistic motors have been adjusted

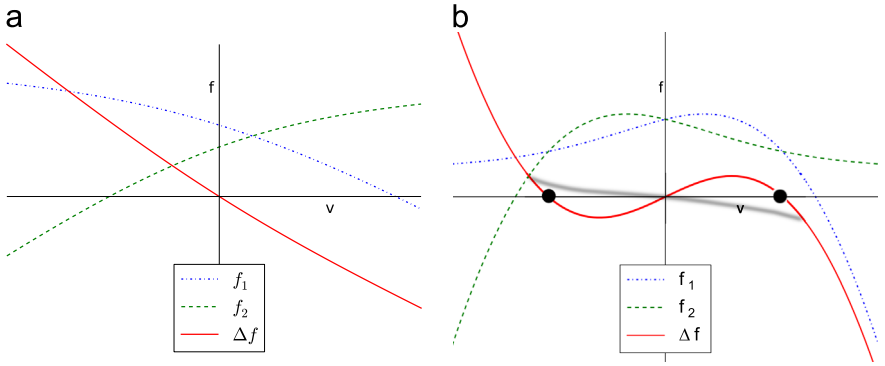

Fig. 3. (a) The average force versus velocity curves, f_1 and f_2, for two species of motors, 1 and 2, that act to antagonize each other. The weighted difference between these two curves, is Δf, with relative concentrations chosen so that they are at the balance point, so that $\Delta f = 0$ for $v=0$. (b) The bistable case where f_1 and f_2 have different functional forms. Now there are two stable states for a given applied force, shown by the filled circles. The curves are done over a sufficiently short time to have two well defined velocities. Over long enough times, fluctuations can allow transitions between these two states. The blurred gray curve is the long time average.

as mentioned above, so that the average force on a microtubule is zero. The position of each motor is random so that even at this concentration, the time averaged force acting on a microtubule will depend on its location, for all realizations of the motor positions. The random placement of motors, implies that there are fluctuations in the net force. If on average, the number of motors acting on a microtubule is N, then we expect this fluctuating time averaged force to have an amplitude that varies proportional to $\sqrt{N}$. This time averaged force will vary slowly as a function of position. This corresponds to having a force correlation function $\langle f_{net}(x) f_{net}(x+\Delta x)\rangle$ that is large over the length of a microtubule. If the microtubule is moved only slightly, most of the same motors will still act upon it, meaning that the force will be highly correlated with its original value. The microtubule has to move its entire length before this time averaged force becomes completely independent of its initial value.

Aside from this time averaged force that is position dependent, we can consider a fixed position and ask how the force varies with time. There will be a substantial variation in the force as a function of time due to the random binding and unbinding of motor ends to the microtubule. Because these events are uncorrelated between motors, the amplitude of these fluctuation will also vary proportional to $\sqrt{N}$.

The above considerations imply that there are two parts to the force exerted on the microtubule, a spatially varying component $F(x)$ and a temporal component $n(t)$. For a fixed microtubule, the total force is the sum of these two terms. The statistical properties of n and F are independent of each other because, for a long microtubule, n is the sum of many independent components and therefore its amplitude is independent of position.

If we now consider a microtubule that is no longer fixed in position, there is a further force due to the drag, as discussed above.

With these three physical effects included, we are now in a position to model this problem more precisely by characterizing the statistical properties of $n(t)$ and $F(x)$, as we now discuss.

2.3. Model as a random walk in random environment

Both in a cell and in the gliding assay experiments, the two motor proteins and microtubules are mixed together in a solution. To model this, we imagine a railroad track with motor proteins randomly placed at every tie. This creates a random environment. A rigid microtubule of length L, is placed on the tracks, and the motors that lie underneath randomly exert a force on the microtubule. With both species of motors randomly exerting forces on the microtubule in opposing directions, the microtubule undergoes random movement on the track given by

$$\gamma \dot{x} = F(x) + n(t), \tag{2}$$

where $F(x)$ is the random static force, $n(t)$ is the time fluctuating force, and γ is the drag coefficient, as discussed above. To be more precise, the left hand side, comes from Eq. (1), where the velocity was maintained at a constant value and was not time varying. Therefore if the velocity of a microtubule varies quickly in time, our argument would be invalid. However we are interested in the behavior near the balance point where velocities are small, and furthermore, the microtubule has many motors that can potentially bind to it, approximately 100 (Tao et al., 2006a). Therefore the fluctuation in the drag coefficient, from one location to another will be small and hence the drag coefficient will only have small variations. On the other hand, at the balance point, the right hand side is purely due to fluctuations. Therefore the error we incur by ignoring changes in γ are of a higher order (in $1/L$) and we are therefore justified in ignoring them. The left hand side contains $v = \dot{x}$, which is the velocity of the center of mass of the microtubule. Eq. (2) is generally known as a Random Walk in a Random Environment (Marinari et al., 1983). The difference between this and previous work lies in the correlations in $F(x)$, which as noted above, is correlated over the length of a microtubule.

Below, we will analyze this equation as follows: The random force $n(t)$ gives an effective temperature for this system. By calculating the statistics of the force the motors exert on the microtubule, this temperature can be determined. Because the force is one dimensional, it is conservative, and a potential energy can always be defined. Note that the existence of a conservative force field, does not preclude dissipative terms in the equations of motion (e.g. Langevin dynamics). By calculating the statistics of $F(x)$, we will know how potential energy correlations behave for length scales much less than L. We can thereby estimate how far a microtubule will move, on average, before being stopped by a potential barrier. Using this, we can make estimates about the oscillatory behavior seen in antagonistic gliding assays.

2.4. Determining forces exerted on the microtubule

One railroad tie will by occupied by either a KLP61F or Ncd motor, where the concentration per site of KLP61F motors is k. If we measure the force the motor exerts over a time much longer than that motor's cycle, we will see a time averaged force of f_{KLP} for one KLP61F motor, or f_{NCD} for one Ncd motor, where $f_{NCD} < 0$. Because the motor exerts a peak force for some time and then exerts no force, the average force is given by

$$f_{KLP} = f_k p_k \tag{3}$$

for KLP61F, and

$$f_{NCD} = f_n p_n, \tag{4}$$

for Ncd, where f_k and f_n are the peak forces exerted by the motors, and $f_n < 0$. p_k and p_n are the probabilities of the motors exerting a force on the microtubule. For simplicity, we will set $p_k = p_n = p$.

The average force exerted by a single motor along the track is determined by the concentrations of the motor species. With a concentration k of KLP61F, the force from one motor site averaged over time and space is given by

$$\langle\langle f\rangle_t\rangle_x = k f_k p + (1-k) f_n p. \tag{5}$$

When this average net force is adjusted experimentally by varying k, the variance of the static force is given by

$$\langle\langle f\rangle_t^2\rangle_x = k(f_k p)^2 + (1-k)(f_n p)^2 = p^2[k f_k^2 + (1-k) f_n^2]. \tag{6}$$

Because a specific motor produces an average force, it follows that at each motor site, the time averaged force is non-zero. Therefore the variance of the time fluctuating force, $n(t)$, is the weighted sum of the variance for each species, and must include terms involving $\langle f\rangle_t$:

$$\langle\langle f^2\rangle_t\rangle_x - \langle\langle f\rangle_t^2\rangle_x = k f_k^2 p(1-p) + (1-k) f_n^2 p(1-p) = p(1-p)[k f_k^2 + (1-k) f_n^2]. \tag{7}$$

Note that this is the variance per site. The variance for the total force on a microtubule of N sites, is N times larger because the forces are all independent.

2.5. Behavior of the potential for distances $\ll L$

Over distances greater than the length of the microtubule, L, the potential will look like a random walk, but to determine if the microtubule will fluctuate about a mean position, as seen experimentally, we must look at the potential at scales $\ll L$. To examine such fluctuations, we must characterize the property of the potential statistically. In this subsection, we do this by considering average properties of the potential. Averages $\langle\cdots\rangle$ are taken here to be over the ensemble of all possible realizations of the random force.

Because $\langle F(x)\rangle = 0$, we expect there to be many zeros for F and the dynamics with $n(t) = 0$ are such that the microtubule will move downhill in potential to arrive at such points. For finite $n(t)$, the microtubule will still on average move towards lower points in potential, but will fluctuate around local potential minima. Therefore we will look at the fluctuations of a microtubule after it has moved into a position, x^*, where the $F(x^*) = 0$. This would represent a local minimum of the potential. The question we are addressing here is: are the fluctuations due to $n(t)$ small enough to confine the microtubule to a certain region? In this section, for simplicity we chose our coordinate system so that $x^* = 0$. Because the force, and therefore the potential, is finite everywhere, and the statistics of the force are translationally invariant, the microtubule cannot be localized to any one region and is expected to eventually move arbitrarily far from an initial point. However we will see that while this is true, the time scale for this happening becomes extremely large, so in practice an experiment will observe confinement of the microtubule to particular region. We will estimate the size of the region that would be explored under normal experimental conditions.

If we move the microtubule a distance, m, we will see a difference in the net force exerted on the microtubule. While most of the microtubule is still being moved by the same motors, a length m of it will be moved by new motors. Therefore, the potential will be changed by some amount proportional to a factor of m.

The net force exerted along the length of the microtubule is given by

$$F(m) = \sum_{i=-L/2+m}^{L/2+m} \eta_i, \tag{8}$$

where η_i is the force exerted at motor site i. Therefore the difference in the net force is

$$F(m) - F(0) = \sum_{i=-L/2+m}^{L/2+m} \eta_i - \sum_{i=-L/2}^{L/2} \eta_i. \tag{9}$$

Eq. (9) simplifies because of cancellations on the right hand side, giving

$$F(m) - F(0) = \sum_{j=0}^{m} \phi_j, \tag{10}$$

where $\phi_i \equiv \eta_{L/2+i} - \eta_{-L/2+i}$ has been introduced to simplify the right hand side of Eq. (9). Note that all ϕ's used below are independent and that $\langle \phi^2\rangle = 2\langle \eta_i^2\rangle$. As discussed above, we are interested in fluctuations about a potential minimum so that $F(0) = 0$.

The potential difference is given by

$$V(x) = -\int_0^x F(x')\, dx'. \tag{11}$$

Turning Eq. (11) into a Riemann Sum, with segments Δ equal to the spacing between motors, gives

$$V(m) = -\Delta \sum_{i=0}^{m} f(x_i) = \Delta \sum_{i=0}^{m} \sum_{j=0}^{i} \phi_j = \Delta \sum_{j=0}^{m} j\phi'_j. \tag{12}$$

where $\phi'_j \equiv \phi_{m-j}$. The ϕ' variables have identical statistics to ϕ, because of the independence of the ϕ's.

To see how the potential scales with m, we look at the average potential difference squared, $\langle (V(m) - V(0))^2\rangle$. To simplify, we will calculate the fluctuations about the minimum, so that $V(0) = 0$. Therefore,

$$\langle (V(m) - V(0))^2\rangle = \langle V(m)^2\rangle = \Delta^2 \sum_{j=0}^{m} \sum_{i=0}^{m} ij \langle \phi'_i \phi'_j\rangle. \tag{13}$$

The correlation function $\langle \phi'_i \phi'_j\rangle$ can be determined from the correlation function for individual motors, $\langle \eta_i \eta_j\rangle$. Since the motors are regularly spaced, the correlation function is given by

$$\langle \eta_i \eta_j\rangle = c\delta_{ij}, \tag{14}$$

because the motors are correlated at distances equal to the motor spacing, and uncorrelated otherwise. The constant c is equal to the variance of the static force, given by Eq. (6). Eq. (14) becomes

$$\langle \eta_i \eta_j\rangle = p^2[kf_k^2 + (1-k)f_n^2]\delta_{ij}. \tag{15}$$

Since $\langle \phi^2\rangle = \langle (\eta_1 + \eta_2)^2\rangle = \langle \eta_1^2\rangle + \langle \eta_2^2\rangle$, the variance of ϕ is twice the variance of η, so that,

$$\langle \phi_i \phi_j\rangle = 2c\delta_{ij}. \tag{16}$$

Inserting Eq. (16) into Eq. (13) and considering large m yields

$$\langle V(m)^2 = 2c\Delta^2 \sum_{i=0}^{m} i^2 = 2c\Delta^2 \int_o^m x^2 dx = \tfrac{2}{3} c\Delta^2 m^3. \tag{17}$$

Therefore, the potential fluctuations for distances $m \ll L$ are proportional to m^3. To calculate how far on average a microtubule will move from a minimum potential, the effective temperature must be determined.

2.6. Determining the effective temperature

Determining the effective temperature of the system will tell us the energy of the system and determine how high the potential barriers must be to keep the microtubule trapped in a potential well. We can do this following the standard argument used to show the Fluctuation Dissipation theorem (Sethna, 2006). Determining the diffusion coefficient, D, will allow us to make use of the Einstein Relation:

$$D = \frac{k_B T}{\gamma}. \tag{18}$$

The force on the microtubule is given by $f(x,t) = \gamma v$, therefore,

$$\int_0^t f(t)\, dt = \gamma(x(t) - x(0)). \tag{19}$$

Therefore,

$$\langle \gamma^2 (x(t) - x(0))^2\rangle = \left\langle \left(\int_0^t f(t')\, dt' \right)^2 \right\rangle = \int_0^t \int_0^t \langle f(t') f(t'')\rangle\, dt\, dt'. \tag{20}$$

The correlation function, $\langle f(t) f(t')\rangle$, can be approximated as a delta function, such that

$$\langle f(t) f(t')\rangle = 2c_0 \tau_d \delta(t - t'), \tag{21}$$

where $c_0 = Lp(1-p)[kf_k^2 + (1-k)f_n^2]$, because the variance per site of the time fluctuating force given by Eq. (7) and τ_d is the decay time of a motor. Substituting Eq. (21) into Eq. (20) gives

$$\int_0^t \int_0^t \langle f(t') f(t'')\rangle\, dt' dt'' = 2c_0 \tau_d t. \tag{22}$$

Setting this equal to the left-hand side of Eq. (20) yields

$$\gamma^2 \langle (\Delta x)^2\rangle = 2c_0 \tau_d t, \tag{23}$$

with the diffusion coefficient defined as $1/2t\langle (\Delta x)^2\rangle$, so that

$$D = \frac{c_0 \tau_d}{\gamma^2}. \tag{24}$$

Using Eq. (24) and the Einstein Relation, Eq. (18) yields an effective temperature:

$$k_B T = \frac{c_0 \tau_d}{\gamma}. \tag{25}$$

Note that both the drag coefficient γ, and c_0 are proportional to L, so that this effective temperature does not depend on the length of the microtubule. We therefore only need to know both γ and c_0 per unit length when calculating this temperature.

2.7. Estimating microtubule fluctuation amplitude

To estimate the distance a microtubule moves before encountering a potential barrier of order k_BT, we set Eq. (17) equal to $(Ak_BT)^2$, where A is a multiplicative factor, giving

$$\langle V^2\rangle = (Ak_BT)^2 = \tfrac{2}{3}c\Delta^2 m^3. \tag{26}$$

Solving for m yields

$$m = \left[\frac{3(Ak_BT)^2}{2c\Delta^2}\right]^{1/3}. \tag{27}$$

Plugging in Eq. (25) yields

$$m = \left[\frac{3\left(A\frac{c_0\tau_d}{\gamma}\right)^2}{2c\Delta^2}\right]^{1/3} = \left[\frac{3\left(\frac{A}{\gamma}p(1-p)[kf_k^2+(1-k)f_n^2]\tau_d\right)^2}{2p^2[kf_k^2+(1-k)f_n^2]\Delta^2}\right]^{1/3}. \tag{28}$$

If we make the further simplifications that the two motor species exert the same peak force f_e, the concentrations of the species are equal, and the probability of a motor exerting a force is $\frac{1}{2}$, then Eq. (28) becomes

$$m = \left[\frac{3\left(A\frac{f_e^2\tau_d}{4\gamma}\right)^2}{\frac{1}{2}f_e^2\Delta^2}\right]^{1/3} \approx \left[\frac{(A^2f_e^2\tau_d^2}{2\gamma^2\Delta^2}\right]^{1/3} \tag{29}$$

According to Tawada and Sekimoto (1991), γ (per unit length) can be approximated as kt, where κ is the effective spring constant of the motor, and t is the characteristic time for the motor to be associated with the microtubule per cycle (Tao et al., 2006b). Since we approximated $\tau_d \approx t$, Eq. (29) becomes

$$m \approx \left[\frac{Af_e}{\sqrt{2}\kappa\Delta}\right]^{2/3}. \tag{30}$$

Using $\kappa \approx 1$ pN/nm (Tao et al., 2006b), $\Delta \approx 50$ nm (Tao et al., 2006a), and $f_e \approx 10$ pN,

$$m \approx \left(\frac{A}{2}\right)^{2/3}. \tag{31}$$

Therefore, to reach a potential barrier of order $10k_BT$, the microtubule would have to move ≈ 3 motor sites, or 0.15 μm.

This is in agreement with the fluctuation size of ≈ 0.2 μm measured in motility assays, as in Fig. 5 from Tao et al. (2006a). Also, it is likely that the potential barrier must be greater than $10k_BT$ to contain the microtubule, thereby giving an estimate closer to the experimental result.

In addition, we can determine how the distance the microtubule moves scales with time. According to Kramer's theory of thermal activation, the time scale t for escaping a potential is proportional to $\exp \Delta V/(k_BT)$ (Kramer, 1940). Since $\Delta V \sim x^{3/2}$, therefore $x \sim \ln t^{2/3}$. Thus, the microtubule can cover a large distance very quickly, but then is trapped in a potential well and restricted to oscillatory motion.

3. Simulations

The analytical work of the last section made assumptions that can be verified by numerical implementation of the underlying model. Our analysis divided up the dynamics into two types of variable: average quantities and noise, the latter being Gaussian and uncorrelated. By implementing the original model numerically, we can test to see to what extent our analysis agrees with simulation. We will see that there is very good agreement between them.

Having established the validity of our analytical approach, Eq. (2), we can do a more quantitative analysis of it by numerical simulation to verify the behavior predicted above. This also leads to a more accurate description of statistical quantities, such as the distribution of fluctuations. In particular, we can calculate the steady state probability of the microtubule's position, and also the distribution of initial distances that it travels before becoming trapped.

In the following, we use units of length so that the distance between adjacent motors is unity.

3.1. Numerical implementation of antagonistic motors

We consider the model in Section 2.3 with one of two possible motor proteins positioned at every tie, with concentrations per site k, and p, as described in Section 2.4.

A single motor can be in two states, attached, or unattached to the microtubule. When it is attached it has a probability per unit time $1/\tau_d$ of detaching. If it is unattached, the probability per unit time of attaching is $1/\tau_a$. Below we show simulation results where these two rates are the same: $\tau_d = \tau_a \equiv \tau$ and with $k = p = 1/2$.

The total force f_{tot}, is obtained by summing the forces over all attached motors. We also assume that each attached motor has an identical linear drag coefficient of unity. The total drag γ is therefore the sum of the drag over all attached motors.

We model the force in the simplest way possible to avoid any effects related to a load dependent detachment rate, by making the forces constant during attachment. We set the peak forces used above to $f_k = -f_n = 1$. The simulation is implemented by integrating this model with a time step $dt = 0.01$. At every step we decide to attach or detach all of the motors according to the probabilities stated above. With the updated state of the motors, we calculate the new total force acting on the microtubule. This is used to get the change in position of the microtubule, $dt\, f_{tot}/\gamma$. When the microtubule shifts by one tie, it is able to attach to a new site on the leading end, and can no longer attach to the last site on the trailing edge.

The corresponding potential of the microtubule can be obtained by first calculating the average total force of a microtubule as a function of position. We chose a microtubule with $N = 100$ sites. We then integrate this force to obtain the potential. A typical potential is shown in Fig. 4(a). Starting with a displacement of 0, the microtubule will move down the potential towards the rectangular region, as shown. With the same forces corresponding to this potential, we ran our simulation to obtain the displacement of the microtubule versus time, Fig. 4(b). The initial transient region is shown in Fig. 4(c). This can be compared to the corresponding experimental results shown in Fig. 1, reproduced here from Tao et al. (2006a).

We quantitatively compare our simulation with our theory in Fig. 4(d). The probability distribution of displacements x, is highly metastable and should be well described by a Gibbs distribution, $p(x) \propto \exp(-V(x)/(k_BT))$. The temperature T was calculated in Section 2.6. Using Eqs. (7) and (25), with the parameters above, $\gamma = L/2$, $p = k = 1/2$, $f_k = f_n = 1$, gives $k_BT = 1$. The dashed curve shows the Gibbs prediction, which agrees well with the probability distribution determined from Eq. (2).

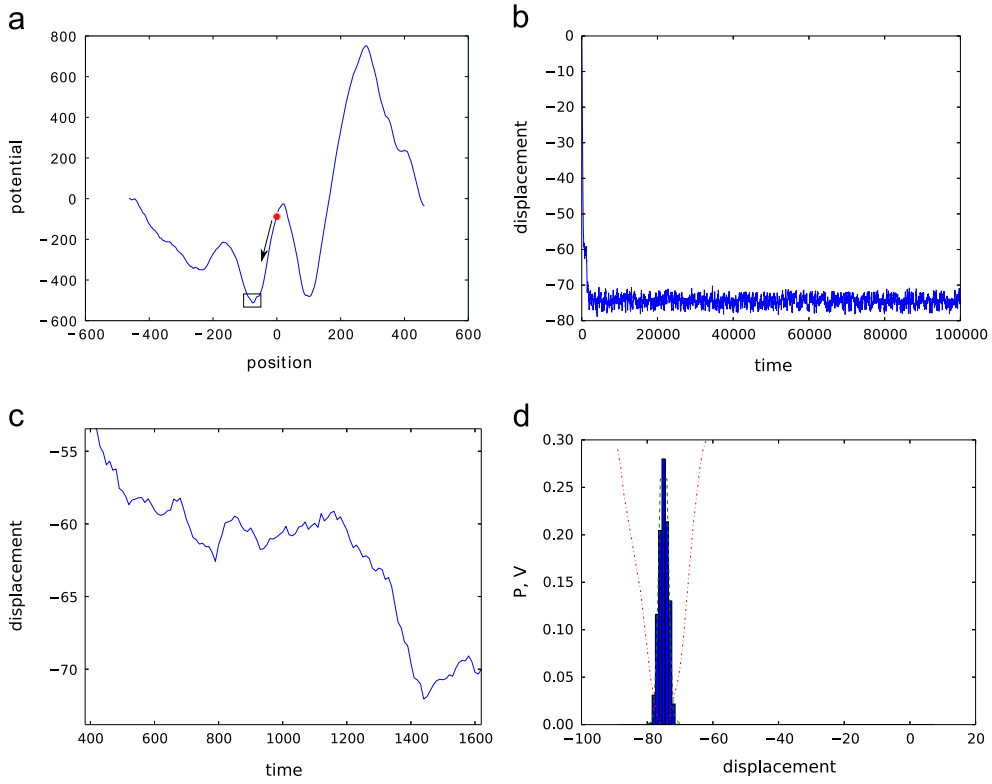

Fig. 4. (a) The computed potential versus displacement for a particular realization of the two antagonistic motor proteins described in Section 3.1. The dot shows the starting position. The arrow points to the final position shown as a rectangle. (b) The displacement as a function of time for a simulation of this system. (c) The initial transient behavior is expanded. (d) The probability distribution of displacements computed from the latter half of the data shown in (b). For comparison, the theoretical prediction from our model is shown with the dashed lines. The two agree well. The potential V from (a) is shown with the dot-dashed line (scale $\times$ 100).

3.2. Numerical implementation of random environment model

The above simulation establishes the validity of our approach Eq. (2), modeling the system as a random walk in a random environment, with specific correlations in the random potential derived above. We now directly simulate Eq. (2) with our derived statistics, to obtain statistical quantities that are hard to obtain analytically.

We consider a force produced by a motor at the ith site, f_i, drawn from a standard normal distribution. The net force acting on a microtubule, $F(j)$, is the sum over L adjacent sites of these random forces, as in Eq. (8). We then linearly interpolate for non-integral values of x to obtain the force at an arbitrary position which gives us the complete force for any value of x. We choose $n(t)$ from a Gaussian distribution with standard deviation C, to describe the system at a temperature T. We solve Eq. (2) by a simple Euler discretization with a time step $dt=0.01$. The noise amplitude is related to the temperature by $C=\sqrt{2T/dt}$. In the simulations below, we chose $N=L=100$, and $k_BT=4.0$.

Fig. 5 shows a single run for one random realization of random forces. The displacement starting from $x=0$ is shown as a function of time in (a). Fig. 5(b) shows the same data rescaled to reveal the behavior of the initial transient. Note that the microtubule moves approximately 35 units before finding a deep potential minimum. Fig. 6 displays the corresponding histogram of microtubule position. The initial transient behavior was not included. The non-Gaussian shape is due to the underlying roughness of the force $F(x)$ and its corresponding potential. For extremely long times, this histogram will change because the microtubule will eventually be able to overcome enormous energy barriers. However the corresponding times for these are exponentially large as discussed in the previous section. Under experimentally reasonable time scales, we expect this kind of histogram to be obtained.

We now probe the behavior of the initial transients, noted above. We ran this simulation 3000 times each with randomly generated forces. Then we computed the initial displacement for each realization by taking the difference between the steady state average position and the initial position. A histogram of these differences is shown in Fig. 7. As is apparent, the displacement in a transient is typically about 100, or the length of the microtubule.

4. Model application to interpolar microtubules during metaphase

We have seen that the effect of antagonistic motors is indeed to lead to a quasi-steady state behavior for gliding assays where microtubules fluctuate in a localized region. However, there is a sizable initial transient displacement before it becomes localized, that appears to be of order the length of the microtubule.

The reason for this relatively large initial transient can be understood from the statistics of random walks. The time averaged net force F, is the sum of the forces of the individual motors, Eq. (8), and the displacement from that point will follow random walk statistics for lengths smaller than the length of the microtubule L as seen from Eq. (9). On average, F will have a magnitude that scales as $\sqrt{L}$. If we are interested in how far a microtubule must travel before $F=0$, then this must be a distance that is proportional to L, because a displacement of this size will typically give rise to a change in force that is also proportional to $\sqrt{L}$.

Now consider the situation of competitive motors on anti-parallel microtubules, interacting with each other as shown in Fig. 8. We can use an analysis similar to our treatment of the gliding assay experiments to understand this situation. This therefore assumes that the positions of motors on the microtubules are fixed. In reality we expect some movement of them as well. Therefore the potential that the

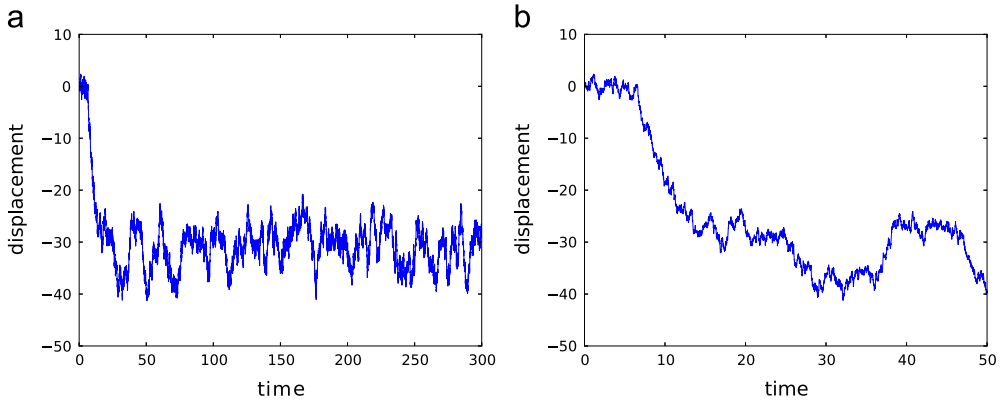

Fig. 5. (a) Displacement versus time for a particular realization of random forces for the random environment model of Section 3.2. (b) Same plot but expanded for short times. Note that initially it moves until it reaches a position which is more favorable "energetically".

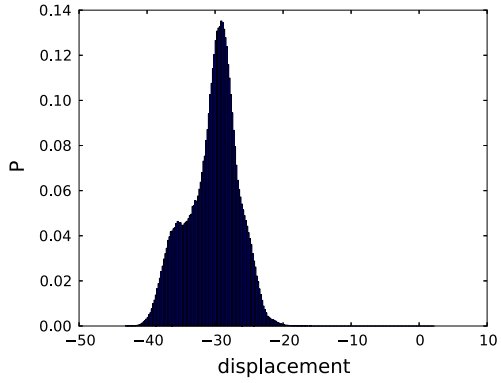

Fig. 6. Histogram of positions for a single realization of the random forces. The initial transient was not included. The system fluctuations are not Gaussian as is expected because the force does not vary linearly with positions. After extremely long times, this distribution must change but this happens so slowly as not to be experimentally relevant.

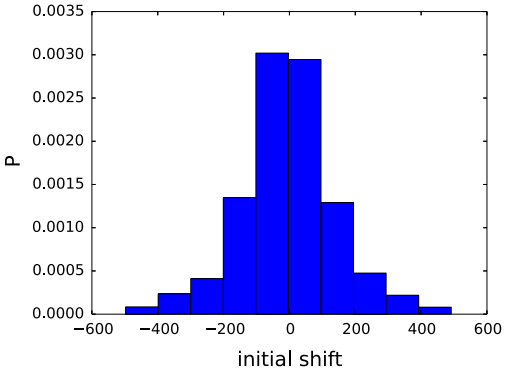

Fig. 7. A histogram of the displacement due to the initial transients. The simulation was run 3000 times and the initial displacements were all computed. The initial displacement was obtained by taking the difference between the steady state average position and the initial position of the microtubule.

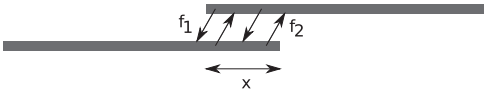

Fig. 8. Two anti-parallel microtubules interacting via two types of antagonistic motors. The motors interact in the region of overlap.

microtubules feel changes in time. The potential will change significantly on a timescale where motors move on the order of the overlap distance between microtubules. The new motor densities that are now connecting the microtubules will then be uncorrelated with their initial value. However the motion of these motors is not known and we will examine the situation where their movement is slow on the timescales of interest.

The motors will only operate in the region where the microtubules overlap, which in Fig. 8 is over a distance of length x, corresponding to $m = x/\Delta$ motors. Eq. (8) is modified to be

$$F(m) = \sum_{i=0}^{m} \eta_i, \tag{32}$$

where $\eta_i = f_{1,i} + f_{2,i}$ is the sum of the effects motors walking on both microtubules. This form is different from the gliding assay case, because now the number of motors included in the sum depends on the overlap distance x. However $F(m)$ is still of the form of a random walk. Therefore the total force is not expected to vanish except possibly at a finite number of random values of x. The microtubules are therefore expected to have transients that are also large, but different than the case of the gliding assays. We would like to know in this situation if the spindle length is maintained at a constant value, that is, if the two microtubules will come to a well characterized equilibrium separation, or if, in fact, they will not do so. We answer this question as follows.

The two microtubules will stop moving, aside from "thermal" fluctuations, only at points where the force $F(x)$ is zero. So it is important to understand where such points lie. F itself has the statistics of a random walk, where in this application, the position of the random walk is in force-space, and time for the random walk becomes the distance of overlap, x. We are interested in starting the microtubules off at some initial x and asking how this will evolve in time. Depending on the sign of F, x will either increase or decrease monotonically until it reaches a zero of F. This problem is equivalent to the first passage time problem of a random walk. In the case where the sign of F is such that the microtubule moves to increasing x, this would be equivalent to a random walk that starts off some distance from zero and asking how long it will take to cross zero. In this case, if the distance of overlap starts out as x_0, it will experience a random force as given in Eq. (32). In the absence of external forces, the two microtubules will slide until they reach an overlap x^* such that $F(x^*) = 0$. As in the gliding assay case, this will typically be a distance of order x_0.

On the other hand, if the sign of F is initially such that the microtubule moves in a direction of decreasing x, then two things can happen. It can reach a zero of F at a point where $x > 0$, or there will be no zeros until $x = 0$. In the latter case, the microtubules slide off of each other. To ascertain the likelihood of this latter possibility, we note again that the statistics of $F(m)$ will be that of a random walk that starts out with $F(0) = 0$. The probability of a

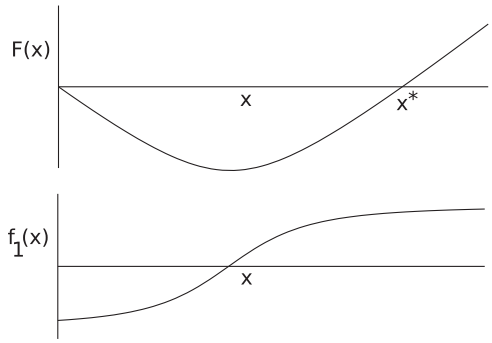

Fig. 9. The total force F, and force density profile f_1 as a function of overlap x of the two antiparallel microtubules caused by a density variation of antagonistic motors as described in the text. Such a deterministic arrangement will lead to a balance point at x^* that will compete with spatio-temporal fluctuations of the two motor species.

random walk of length m starting at the origin but never passing through zero can be obtained (Chandrasekhar, 1943). For example, if the motor spacing $\Delta = 50$ nm and the overlap $x = 1$ μm, then we are asking for the probability that a random walk of length 20 never passes through its starting position. In that case that probability is about 0.18. This means the in this example, there is a 0.18 probability that the two microtubules will separate. Because in reality, there are many microtubules involved in the spindle, this means that many overlapping microtubules will be pushed away from each other so that they no longer overlap. Conversely, many others will increase from an overlap of 1 μm to greater than 2 μm.

Therefore this model of motor association during prometaphase, does a somewhat imperfect job of maintaining spindle length. One simple way to improve its efficacy is to have a *gradient* in motor concentrations. In this case in Eq. (32), instead of the forces f_1 and f_2 being random variables with a mean zero, we say that the local motor concentrations are not at the balance point, so that there is a net time averaged force that varies deterministically with position. Let us further assume that the concentration profile is the same for both microtubules. Then the corresponding force densities $f_1(x)$ and $f_2(x)$, will give equal contributions to the net force that the microtubules exert on each other.

$$F(x) = 2\int_0^x f_1(x')\,dx'. \tag{33}$$

Fig. 9 displays a force density profile that has the right properties. $f_1(x)$ starts off negative, close to $x=0$, meaning that near the tip of the microtubules, the motors have the net effect of pulling each other closer together. At some point the sign of $f_1(x)$ changes and motors in that region predominantly pull the microtubules apart. The net force due to all the motors as a function of overlap, $F(x)$ is obtained by integrating $f_1(x)$. The equilibrium overlap x^* is when $F(x^*) = 0$. By adjusting the profile of motor concentrations, x^* can be shifted.

4.1. Strength of concentration imbalance

One caveat that should be mentioned is that if the motor concentration gradients are too weak, then the microtubules will become stuck due to the randomly fluctuating force. Without a strong enough bias due to motor concentration variation, the extremely jagged random environment will prevent microtubules from sliding to the equilibrium point x^*. We now consider the minimum size of this concentration variation necessary to overcome the random static forces.

The force in Fig. 9 is linear around the equilibrium point x^*, and is of the form of Hooke's law: $F = -\kappa x$, where x is measured relative to x^*. The maximum value that κ can take can be determined by the extreme case where the force on the microtubule changes from 0 to f_e within one motor spacing Δ. If this change occurs over a width of n motors instead, we can write $\kappa = f_e/(n\Delta)$. We wish to determine the maximum value of n that is consistent with the microtubules being able to slide relative to each other. The potential corresponding to Hooke's law is $U = \kappa x^2/2$. Compared with the statistics of the random potential, Eq. (26), where $V \propto x^{3/2}$, we see that for small enough x, the random force dominates, but when x becomes sufficiently large, Hooke's law prevails. If the crossover occurs at too large a value of x, then the system will become trapped in some local random minimum and not be able to move closer to x^*. To determine this crossover, we equate the standard deviation of the fluctuation in the random potential, given by Eq. (26), with the Hookean potential. In terms of $m = x/\Delta$, we obtain

$$n^2 = \frac{3 f_e^2 m}{8\ c}, \tag{34}$$

where the force variance c is given in Eq. (15). To estimate the value of n, we take $p = 1/2$, and $f_k = f_n = f_e$. This gives $n^2 = (3/2)m$. Experimentally in a gliding assay, it was found that the fluctuations in m where approximately 4. This means that we expect that n should be in the range 2–3, in order for the microtubules to slide within the experimental time scale.

This small value of n is consistent with the fact that at the balance point, the fluctuations in position of a microtubule in a gliding assay are small. The spacing between motors, in these assays, is presumably not identical to interpolar microtubules in the spindle but they are believed to be plausibly similar (Tao et al., 2006a; Brust-Mascher et al., 2004).

5. Conclusion

By means of a fairly general analysis, making few assumptions, we have seen that the motion of microtubules in an antagonistic motility assay near the balance point is well described by a random walk in a random environment (Marinari et al., 1983), but with large correlations in the static random force. The connection does not depend on a detailed model of the motors. The force velocity curves of the motors near the stall point, $v = 0$, only come into play to give a drag coefficient for the microtubule. The results found are in reasonable agreement with the fluctuations observed in microtubule positions seen in experiments (Tao et al., 2006a). However the model also predicts that microtubules will slide of order their own distance before getting badly trapped, as seen in the initial transient data.

There is substantial similarity between these gliding assay experiments and models for what occurs *in vivo* during prometaphase, with KLP61F and Ncd motors antagonizing each other in mitotic spindles (Tao et al., 2006a; Civelekoglu-Scholey et al., 2010). However, although random force fluctuations correctly predict that these motors will act to inhibit variations in spindle length, they also do so imperfectly. Antiparallel interpolar microtubules will have initial transients where they slide of order their own length, or sometimes completely disassociate. It appears that such variations are within the error bars of experimental observation however. But, to circumvent these fluctuations, it is possible that the cell sets up a gradient in motor density during prometaphase, thereby restricting the mitotic spindle to confined movements in a potential well. Further observations of the densities of motors *in vivo* could lend a great deal to further understanding of this situation.

Acknowledgments

This material is based upon work supported by the National Science Foundation under Grant CCLI DUE-0942207.

References

Badoual, M., J̈licher, F., Prost, J., 2002. Bidirectional cooperative motion of molecular motors. Proc. Natl. Acad. Sci. U.S.A. 99, 6696–6701.
Brust-Mascher, I., Scholey, J.M., 2002. Microtubule flux and sliding in mitotic spindles of Drosophila embryos. Mol. Biol. Cell 13, 3967–3975.
Brust-Mascher, I., Civelekoglu-Scholey, G., Kwon, M., Mogilner, A., Scholey, J.M., 2004. Model for anaphase B: role of three mitotic motors in a switch from poleward flux to spindle elongation. Proc. Natl. Acad. Sci. U.S.A. 101, 15938–15943.
Chandrasekhar, S., 1943. Stochastics problems in physics and astronomy. Rev. Mod. Phys. 15, 1–85.
Civelekoglu-Scholey, G., Tao, L., Brust-Mascher, I., Wollman, R., Scholey, J.M., 2010. Prometaphase spindle maintenance by an antagonistic motor-dependent force balance made robust by a disassembling lamin-B envelope. J. Cell Biol. 188, 49–68.
Cole, D.G., Saxton, W.M., Sheehan, K.B., Scholey, J.M., 1994. A "slow" homotetrameric kinesin-related motor protein purified from Drosophila embryos. J. Biol. Chem. 269, 22913–22916.
Cottingham, F.R., Gheber, L., Miller, D.L., Hoyt, M.A., 1999. Novel roles for *Saccharomyces cerevisiae* mitotic spindle motors. J. Cell Biol. 147, 335–350.
Duke, T., 2002. Push or pull? Teams of motor proteins have it both ways. Proc. Natl. Acad. Sci. U.S.A. 99, 6521–6523.
Enos, A.P., Morris, N.R., 1990. Mutation of a gene that encodes a kinesin-like protein blocks nuclear division in A. nidulans. Cell 60, 1019–1027.
Gilboa, B., Gillo, D., Farago, O., Berheim-Groswasser, A., 2009. Bidirectional cooperative motion of myosin-II motors on actin tracks with randomly alternating polarities. Soft Matter 5, 2223–2231.
Guérin, T., Prost, J., Martin, P., Joanny, J.F., 2010. Coordination and collective properties of molecular motors: theory. Curr. Opin. Cell Biol. 22, 14–20.
Heck, M.M., Pereira, A., Pesavento, P., Yannoni, Y., Spradling, A.C., Goldstein, L.S., 1993. The kinesin-like protein KLP61F is essential for mitosis in Drosophila. J. Cell Biol. 123, 665–679.
Jülicher, F., Prost, J., 1995. Cooperative molecular motors. Phys. Rev. Lett. 75, 2618–2621.
Jülicher, F., Prost, J., 1997. Spontaneous oscillations of collective molecular motors. Phys. Rev. Lett. 78, 4510–4513.
Kramer, H.A., 1940. Brownian motion in a field of force and the diffusion model of chemical reaction. Physica 7, 284–304.
Marinari, E., Parisi, G., Ruelle, D., Windey, P., 1983. Random walk in a random environment and 1/f noise. Phys. Rev. 50, 1223–1225.
Saunders, W.S., Hoyt, M.A., 1992. Kinesin-related proteins required for structural integrity of the mitotic spindle. Cell 70, 451–458.
Sawin, K.E., LeGuellec, K., Philippe, M., Mitchison, T.J., 1992. Mitotic spindle organization by a plus-end-directed microtubule motor. Nature 359, 540–543.
Sethna, J.P., 2006. Statistical Mechanics Entropy, Order Parameters and Complexity. Oxford University Press, Great Britain, p. 227.
Sharp, D.J., Yu, K.R., Sisson, J.C., Sullivan, W., Scholey, J.M., 1999. Antagonistic microtubule-sliding motors position mitotic centrosomes in Drosophila early embryos. Nat. Cell Biol. 1, 51–54.
Straight, A.F., Sedat, J.W., Murray, A.W., 1998. Time-lapse microscopy reveals unique roles for kinesins during anaphase in budding yeast. J. Cell Biol. 143, 687–694.
Tao, L., Mogilner, A., Civelekoglu-Scholey, G., Wollman, R., Evans, J., Stahlberg, H., Scholey, J.M., 2006a. A homotetrameric kinesin-5, KLP61F, bundles microtubules and antagonizes Ncd in motility assays. Curr. Biol. 16, 2293–2302.
Tao, L., Mogilner, A., Civelekoglu-Scholey, G., Wollman, R., Evans, J., Stahlberg, H., Scholey, J.M., 2006b. Supplemental data to a homotetrameric kinesin-5, KLP61F, bundles microtubules and antagonizes Ncd in motility assays. Curr. Biol. 16, 2293–2302.
Tawada, K., Sekimoto, K., 1991. Protein friction exerted by motor enzymes through a weak-binding interaction. J. Theor. Biol. 150, 193–200.